Magnetic ordering of nanocluster ensembles promoted by electronic substrate-mediated interaction: *Ab initio* and kinetic Monte Carlo studies

P. A. Ignatiev,[1] N. N. Negulyaev,[2] A. S. Smirnov,[3] L. Niebergall,[1] A. M. Saletsky,[3] and V. S. Stepanyuk[1,*]
[1]*Max-Planck-Institut für Mikrostrukturphysik, Weinberg 2, D-06120 Halle, Germany*
[2]*Fachbereich Physik, Martin-Luther-Universität Halle-Wittenberg, Friedemann-Bach-Platz 6, D-06099 Halle, Germany*
[3]*Faculty of Physics, Moscow State University, 119899 Moscow, Russia*
(Received 6 May 2009; revised manuscript received 18 September 2009; published 12 October 2009)

By means of *ab initio* calculations and kinetic Monte Carlo simulations we demonstrate that the indirect interaction mediated by conduction electrons of nonmagnetic metallic substrate could stabilize magnetic order of ensemble of magnetic nanoclusters at high temperatures. We especially focus on the conditions necessary for such magnetic ordering.

DOI: 10.1103/PhysRevB.80.165408 PACS number(s): 73.20.−r, 72.10.Fk, 75.75.+a, 02.70.Uu

I. INTRODUCTION

Understanding of magnetic behavior of atomic-scale systems has recently become one of the major challenges[1–5] due to wide range of applications of such systems in modern magnetic storage technology. Increasing capacity of storage devices results in the miniaturization of their elements—nanoclusters or nanodots constructed of magnetic atoms. The magnetic anisotropy energy (MAE) of small nanostructures is, however, insufficient to hinder the effect of thermal fluctuations[6] so the blocking temperature at which these fluctuations destroy a magnetic order of an ensemble of magnetic units is usually far below the room temperature (RT).[7,8] The way to stabilize the magnetic order is to exploit long-range interactions between magnetic nanostructures.[4]

There are two obvious candidates to the role of stabilizing force:[9–16] the dipolar interaction and the indirect substrate-mediated interaction, whose behavior depends on the substrate electronic properties.[16–21] Already first theoretical studies on magnetic particles embedded into the nonmagnetic metallic host demonstrated the complex interplay of both interactions with the size of interacting nanostructures and the distance between them.[16,17] It was actually predicted that it is possible to enhance one of the interactions by deliberate choice of these characteristics.[17] A set of recent experimental works confirmed this proposal. In particular, RT magnetic ordering stabilized by dipolar interaction has been recently revealed in Co films on Cu(001).[13] Since the dipolar interaction decays fast with the separation between magnetic units, the magnetic ordering at temperatures approaching the RT appears only at high Co coverages, i.e., when magnetic units start to overlap. Recent experiments performed by means of scanning tunneling microscopy and magneto-optical Kerr effect techniques in the group of Shen from Oak Ridge National Laboratory[14,15] have clearly indicated that *indirect substrate-mediated interaction* can cause the high-temperature ferromagnetism at large separations between magnetic Fe units on a Cu(111) substrate. Despite the fact that the key point of our research was inspired to a great extent by results of Shen *et al.*,[14,15] we do not aim to explain these studies in details. The reason behind this is the lack of detailed information on the experimental results[14,15] such as nanodot MAE distributions and dot-dot separation distribution.

We give in this paper a clear *theoretical* evidence that substrate-mediated interaction between nanoclusters could lead to high-temperature ferromagnetism of cluster ensembles. In our study we address a question, which conditions must be satisfied to induce such a ferromagnetic ordering. To do it we combine two theoretical approaches. The strength of the indirect substrate-mediated exchange interaction is obtained by means of the *ab initio* Korringa-Kohn-Rostoker (KKR) method. The magnetic ordering (i.e., blocking temperature) of an ensemble is studied using kinetic Monte Carlo (kMC) simulations. As an example, we concentrate on magnetic behavior of Fe nanoclusters (and nanodots) on Cu(111).

The rest of our paper is organized as follows. Section II is devoted to the *ab initio* calculations of the exchange interaction between magnetic nanoclusters on a nonmagnetic metallic substrate. In Sec. III, we describe kMC simulations of the magnetization dynamics and present our data on blocking temperatures of different ensembles of magnetic units.

II. EXCHANGE INTERACTION BETWEEN NANOCLUSTERS

A. KKR method

The strength of the indirect substrate-mediated exchange interaction between magnetic units on a nonmagnetic noble-metal substrate supporting surface-state electrons is calculated within the formalism of the density-functional theory in the local spin-density approximation implemented in the framework of the KKR Green's function method.[22–27] This method describes ground-state properties by means of the Green's function of a system. The key point of the KKR method is that the Green's function $\hat{G}_1(\varepsilon)$ of a perturbed system can be expressed from the Green's function $\hat{G}_0(\varepsilon)$ of the reference system by means of the Dyson equation $\hat{G}_1(\varepsilon)=\hat{G}_0(\varepsilon)+\hat{G}_0(\varepsilon)\hat{T}(\varepsilon)\hat{G}_0(\varepsilon)$, where $\hat{T}(\varepsilon)$ is so-called transition matrix (or T matrix) relating the states $|\Psi_1\rangle$ of perturbed system to the states $|\Psi_0\rangle$ of the unperturbed one. T matrix is defined as $\Delta\hat{V}|\Psi_1\rangle=\hat{T}(E)|\Psi_0\rangle$, where $\Delta\hat{V}$ is a perturbing potential. The Dyson equation can be formulated in terms of any reference system so it is possible to introduce

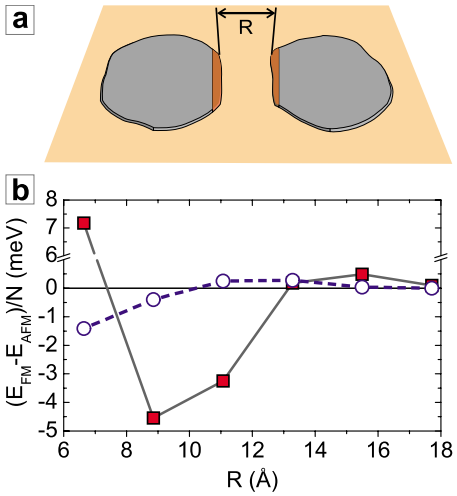

FIG. 1. (Color online) (a) Two clusters on Cu(111) surface. Dark red stripes show the clusters edges governing the substrate-mediated interaction between clusters. (b) Exchange interaction between two parallel Fe wires divided by the total number of atoms in a chain N in the limit of long chains ($N \gg 1$). Circles and dashed lines demonstrate the exchange interaction between two adchains, squares, and solid lines—between two embedded chains.

impurities iteratively. In our case, we first calculate an infinite Cu crystal as a perturbation of free space; then we treat a surface as a two-dimensional perturbation of a crystal; and finally nanostructures on surfaces are considered as a real-space perturbation of an infinite surface. Particular representations of the Green's functions of the system are formulated with the help of multiple-scattering theory.[22,25,27] The KKR formalism provides an easy way to account for the changes in the integrated density of states (i.e., changes in energies) between the perturbed and the reference systems, $\Delta\rho(E) = 1/\pi\ \mathrm{Im}[\mathrm{Tr}(\ln \hat{T})]$. We use this formula (known as Lloyd's formula) to calculate the interaction energies.[26–30] Such an approach accounts both for indirect interactions mediated via bulk states and via surface states. The atomic relaxations are not taken into account in our calculations.

B. Exchange interaction between the borders of nanoclusters

Let us determine how strong exchange interactions mediated by substrate conduction electrons can be. To do it we consider two arbitrary magnetic Fe clusters with smooth borders separated by distance R, as it is sketched in Fig. 1(a). Straightforward *ab initio* treatment of such a system is possible only for clusters comprised of tenth of atoms so the exchange interaction between larger nanostructures should be calculated by means of some approximation. Conduction electrons scattered at each magnetic cluster interfere with each other. Since scattering phase shifts for majority and minority electrons are different, energies of two systems with parallel and antiparallel alignment of magnetic moments of clusters are different.[30] Scattering of conduction electrons is determined mainly by the interface atoms of clusters.[31] Such areas are highlighted in Fig. 1(a) by dark red stripes. As a first approximation the exchange interaction between Fe

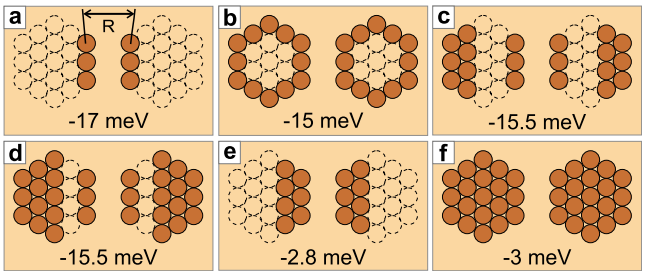

FIG. 2. (Color online) Exchange interactions for the partially filled hexagonal Fe clusters embedded into the surface layer of Cu(111) for separation $R=9$ Å. Dark red circles correspond to Fe atoms and empty circles to substrate Cu atoms.

clusters can be described by the exchange interaction between two parallel monatomic Fe chains of the length N simulating edges of two clusters.

The exchange interaction per chain atom $E_{ex/N}$ for $N \gg 1$ rapidly converge to a limit demonstrated in Fig. 1(b) with circles and dashed line. One can see that the absolute value of $E_{ex/N}$ at $R \gtrsim 9$ Å does not exceed 0.5 meV. Typically, lateral size of a nanoscale magnetic unit is about 2–3 nm,[7,14,15,32] which corresponds to the chain length $N \simeq 10$. The exchange interaction between such chains is $E_{ex/N} \cdot N < 5$ meV. Evidently, this interaction energy is too small to induce ferromagnetic ordering at high temperatures.[3] Brovko *et al.*[30] have recently demonstrated that the exchange interaction can be significantly enhanced by filling the space between magnetic adatoms by the host material. This effect can be explained by the enhanced density of conduction electrons in the spacer between two impurities. Following this hint, we have computed the normalized exchange interaction $E_{ex/N}$ between two long embedded monatomic Fe chains separated by distance R. The result is presented in Fig. 1(b) with squares and solid lines. The exchange interaction at intermediate distances is one order stronger than in the case of adchains and reaches −4.5 meV per atom for $R=9$ Å. For two chains consisting of $N=10$ atoms $E_{ex/N} \cdot N = 45$ meV.

C. Importance of a cluster structure

It is clear that the approximation which is used to estimate the exchange interaction between two embedded clusters is rather crude. To check its relevance we study the impact of the inner cluster atoms on the magnitude of exchange interaction, i.e., consider a set of partially filled pseudomorphic Fe nanoclusters incorporated into the topmost Cu layer at $R=9$ Å, as it is shown in Fig. 2. Since the exchange coupling between adstructures is one order smaller than between embedded ones (Fig. 1), we focus further on embedded clusters. The data provided in Fig. 2 clearly demonstrate two basic features: (i) exchange interaction between nanoclusters is determined by the scattering at the two outermost atomic rows of each cluster; (ii) the second atomic row quenches the exchange interaction [compare Figs. 2(a)–2(d) with Figs. 2(e) and 2(f)]. This quenching can be explained by the difference between phases of electrons backscattered at the first and the second rows of the nanocluster. Indeed, the Fermi wavelength of Cu bulk electrons is 4.62 Å and the distance

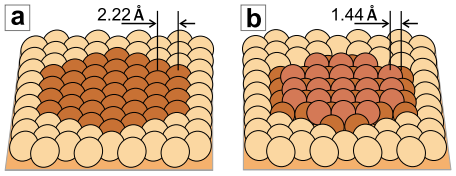

FIG. 3. (Color online) (a) Pseudomorhic fcc Fe nanocluster. The distance between atomic rows is 2.22 Å. (b) Two bottom layers of a bulk Fe nanodot (bcc-like Fe nanocluster). The horizontal separation between atomic rows is 1.44 Å.

between two Fe rows in our model is ~2.22 Å [Fig. 3(a)] so the phase shift is $\sim 0.96\pi$ and two backscattered waves cancel each other.

Obviously, the structure of the magnetic nanocluster is of a great importance for the indirect substrate-mediated interaction. Fe nanoparticles often have a bcc structure,[14,15,33] which of course does not match the Cu fcc substrate, as it is shown in Fig. 3(b). Such a complicated arrangement of the substrate and the nanoparticle atoms makes impossible direct *ab initio* treatment of this system. Nevertheless, some general conclusions can be delivered. The phase shift between electrons backscattered at two atomic planes of a bcc nanocluster is equal to $\simeq 0.6\pi$ and the net backscattered wave is even amplified. This value can be estimated from the distance of 1.44 Å between {100} Fe atomic planes [Fig. 3(b)]. Thus, the exchange interaction presented in Fig. 1(b) with solid line could be used as a reasonable estimation of the real exchange coupling between two buried Fe clusters having bcc structure.

To avoid possible confusions we want to stress that the above-mentioned reasoning on importance of a cluster structure is crucial for bulk states with the Fermi wavelength of 4.62 Å. Such an interaction rapidly decays and starting from separations of 10–20 Å is exceeded by the interaction mediated by the surface state. This parabolic state has much larger Fermi wavelength of 28 Å so there is no destructive interference between electrons scattered at the first and at the second atomic rows and one can consider only one row. The distance at which the surface state begins to play the key role significantly depends on the particular system. For instance, nanoclusters on a surface better scatter surface-state electrons and are less coupled to bulk states than their embedded counterparts. As a result the interaction between adstructures at separations around 10–20 Å is mostly determined by the surface state, however it is not the case for the embedded structures. The smaller magnitude of the interaction via surface state at separations about 10 Å is determined by the smaller density of surface-state electrons with respect to the density of bulk states.[30] Finally, relaxations of adclusters on surfaces increase coupling between surface and bulk states and the ratio of the backscattered surface states participating in the indirect interaction is, therefore, decreased. This, according to our calculations, results in small reduction in the magnitude of the indirect interaction.

D. Importance of ensemble layout

According to our results presented in Fig. 1(b) the blocking temperature is expected to be the highest if (i) all the nanoclusters are partially embedded into the substrate and (ii) their borders are separated by 9 Å. The first condition could be satisfied if the annealing of the sample at room or higher temperature is involved because emission of Cu atoms from the substrate and from the step edges becomes possible.[34] The expelled substrate atoms diffuse across the surface and, since Fe-Cu interaction is stronger than the Cu-Cu one,[35] they attach to Fe nanodots forming rims around them. As a result, nanodots could be partially embedded into the substrate.

To check whether the second condition on the possibility of cluster-cluster separations of 9 Å within a cluster ensemble could be satisfied, we analyzed the ensemble of Fe nanodots from Fig. 1(a) of Ref. 15. We considered that dots are neighbors (i.e., interact with each other) if the separation between their borders is less than 1.5 nm. Magnetic units without neighbors cannot participate in the magnetic ordering of an ensemble since exchange interaction between such clusters is small [Fig. 1(b)], i.e., ferromagnetic behavior of the whole ensemble is determined by units which interact with at least one neighbor. We have found that in the analyzed experimental structure [Fig. 1(a) of Ref. 15] $\simeq$20% of units have no neighbors, $\simeq$50%—one neighbor, and $\simeq$30%—larger number of neighbors. For the random distribution these values are different ($\simeq$45%, $\simeq$40%, and $\simeq$15%). This indicates that in the analyzed experimental structure the distribution of nanodots on a surface is not random.

The physical mechanism responsible for such a self-ordering could be related to the surface-state-mediated long-range interaction which has its first minimum on Cu(111) at ~10 Å.[26,36,37] Recent experimental studies by Nanayakkara *et al.*[38] have surprisingly demonstrated that surface state governs self-assembly of large atomic clusters at 600 K. The most probable separation between the borders of Br nanoislands grown on Cu(111) is close to ~10 Å.[38] Manai *et al.*[39] have reported on the formation of equilateral triangular clusters stabilized at RT by the Rh(111) surface state. Gabl *et al.*[40] have recently demonstrated that repulsive interaction of 20–30 meV mediated by surface-state affect self-assembly of silver nanoclusters on carburized W(110) at $T>300$ K. The surface-state-mediated interaction between Fe nanoclusters has been revealed in our *ab initio* calculations as well. If $E_{\uparrow\uparrow}$ is the energy of two adchains with parallel alignment of magnetic moments, $E_{\uparrow\downarrow}$—with antiparallel alignment, E_0—of the single adchain, then the interaction energy can be calculated as $E_{inter}=\min(E_{\uparrow\uparrow},E_{\uparrow\downarrow})-2E_0$. Figure 4 demonstrates the normalized long-range interaction between two parallel Fe adchains in the ground-state magnetic configuration calculated according to this formula as a function of separation R. The interaction energy of two adchains consisting of $N=10$ atoms at $R=9$ Å equals approximately −20 meV and is comparable with $k_BT\simeq 26$ meV at $T=300$ K, where $k_B=0.086$ meV/K is the Boltzmann constant. Figure 4 clearly indicates that not all the separations are equivalent, the most probable separation between the magnetic units is about 9 Å. This conclusion is not altered if two embedded chains are considered [Fig. 4]. The substrate-mediated long-range interaction between them is even stronger than in the case of supported ones.

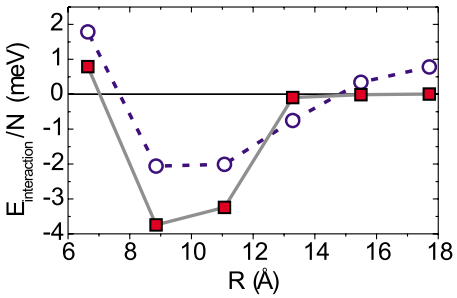

FIG. 4. (Color online) The normalized substrate-mediated long-range interaction between two Fe adchains (circles, dashed lines) and two embedded chains (squares, solid lines) in ground-state magnetic configurations.

III. MAGNETIZATION DYNAMICS

A. Kinetic Monte Carlo model

A realistic insight into the magnetization dynamics of an ensemble of magnetic nanodots implies real-time treatment of a system. Our study of magnetization dynamics was performed by means of kMC method proposed by Li and Liu.[41] Below we briefly highlight the most important points of this technique.

Each nanodot can be considered as a single magnetic domain,[14,15,32] which entirely reverse its magnetization direction at the same instant. It is possible, thus, to treat in our kMC simulations real nanodots as an ensemble of units with magnetic moments $\mu \mathbf{s}_i$, where vector $\mathbf{s}_i$ ($|\mathbf{s}_i|=1$) points the direction of the magnetic moment of an individual nanodot i and the magnetic moment μ of each unit is equal to the net magnetic moment of a typical nanodot.[13] Magnetization dynamics of such a system can be described by the Hamiltonian of the classical Heisenberg model,[41]

$$H = -\sum_{i>j} J_{ij}(\mathbf{s}_i \cdot \mathbf{s}_j) - K\sum_i (\mathbf{e} \cdot \mathbf{s}_i)^2 - \mu\sum_i (\mathbf{B} \cdot \mathbf{s}_i), \quad (1)$$

where J is the exchange energy, K is the energy of on-site magnetic anisotropy, and $\mathbf{B}$ is the external magnetic field aligned parallel to the easy out-of-plane magnetization axis $\mathbf{e}$, $|\mathbf{e}|=1$. It is postulated that directions $\mathbf{s}_i$ of magnetic moments have two metastable states within our model: the first is parallel to $\mathbf{e}$ and the second is antiparallel to $\mathbf{e}$. Such a suggestion implies an Ising-type approach to description of the magnetization dynamics of an ensemble of magnetic units.

Let us now consider a flip of magnetic moment $\mathbf{s}_i$ from the initial metastable state $\mathbf{s}_{i,0}=-\mathbf{e}$ with energy $E_0^{(i)}$ to the final metastable state $\mathbf{s}_{i,1}=\mathbf{e}$ with energy $E_1^{(i)}$. Kinetics of forward and reverse transitions is described by the energy barriers $\Delta E_{0\to 1}^{(i)}$ and $\Delta E_{0\leftarrow 1}^{(i)}$ between two metastable states. To calculate them we follow the way proposed by Li and Liu.[41] The direction of magnetic moment $\mathbf{s}_i$ is rotated from initial metastable state to the final one so the $s_i=(\mathbf{s}_i \cdot \mathbf{e})$ continuously runs through the interval $[-1.0,\ldots,1.0]$ for the forward transition or through $[1.0,\ldots,-1.0]$ for the backward one. It is very important to note that such a transition not necessarily posses a maximum energy at $s_i \in (-1.0,\ldots,1.0)$. The existence of the barrier is determined by the following condition. If $2K>|h_i|$, where $h_i=\mathbf{s}_i(\Sigma_j J_{ij}\mathbf{s}_j+\mu\mathbf{B})$, then the both forward and reverse transition barriers exist and could be calculated as[41]

$$\Delta E_{0\to 1}^{(i)} = (2K+h_i)^2/4K. \quad (2)$$

The frequency rate of such transition is calculated by means of Arrhenius law,[41]

$$\nu = \nu_0 \exp(-\Delta E_{0\to 1}^{(i)}/k_B T). \quad (3)$$

If $2K \le |h_i|$ then there is no transition state barrier [see possible scenarios in Figs. 1(d) and 1(e) of Ref. 41], and following the proposal by Li and Liu[41] we apply Glauber dynamics[42] in order to compute exponential factor of the frequency rate,

$$\nu = \nu_0 \frac{\exp(-\Delta E^{(i)}/k_B T)}{1+\exp(-\Delta E^{(i)}/k_B T)}, \quad (4)$$

where $\Delta E^{(i)}=E_1^{(i)}-E_0^{(i)}$ is the difference between final and initial states of the system. The described model has been successfully applied for the simulations of the magnetization response of monatomic Co chains on a stepped Pt(997) surface at different temperatures.[41]

It is worth to note that the Metropolis algorithm[43] can be used instead of scheme by Glauber[42] for calculations of frequency rates in absence of a transition state barrier (i.e., when condition $2K \le |h_i|$ is satisfied),

$$\nu = \nu_0 \min\{1, \exp(-\Delta E^{(i)}/k_B T)\}. \quad (5)$$

All the results on magnetization dynamics obtained for the same sets of parameters K and J by means of Glauber and Metropolis expressions (4) and (5) are practically the same.

Transition rates [Eqs. (3) and (4)] [or Eq. (5)] are then used to calculate the real-time increment of each Monte Carlo step. If the total number of units in a system is equal to N, then for every kMC step N different flips with the rates $\{\nu_i\}_{i=1,\ldots,N}$ are possible. The time increment τ corresponding to one step of the kMC algorithm is computed using the following expression:[44]

$$\tau = -\ln U/\sum_{i=1}^{N} \nu_i, \quad (6)$$

where U is random number with a uniform distribution in the interval (0, 1).

B. Simulation results

In this section we present the results of the kMC simulations of magnetization dynamics of an ensemble of magnetic units. For the simulations we derive some characteristics of a nanodot assembly from the studies of Torija *et al.*, [Fig. 1(a) in Ref. 15]. Nevertheless our results still cannot serve for the quantitative description of these experiments due to the lack of knowledge of other important information: exact shape of nanodots, distribution of MAE within a nanodot, and unit-unit separation distribution.

According to the Fig. 1(a) in Ref. 15 we consider that magnetic units are distributed with a surface density of 1.2

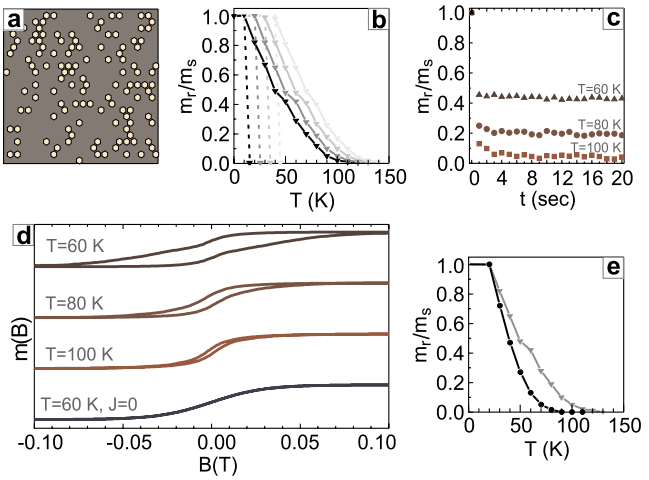

FIG. 5. (Color online) (a) An example of quasirandom distribution of nanodots, with a preferable separation between the nearest borders equal to 9 Å. The field has dimensions 100×100 nm^2. (b) Relative remanent magnetization m_r/m_s as a function of temperature, where m_r is a remanent magnetization at $t=20$ s and m_s is the initial magnetization at $t=0$ s. Solid (dashed) curves are plotted for $J=50$ meV ($J=0$ meV). Black, gray, light gray, and light-light gray curves correspond to $K=30$, 50, 70, and 90 meV, respectively. (c) Time dependence of remanent magnetization of the ensemble for $K=50$ meV at different temperatures: 60, 80, and 100 K. (d) Hysteresis loops calculated for $K=50$ meV at $T=60$, 80, and 100 K. The bottom loop is plotted for $J=0$ meV and $K=50$ meV at $T=60$ K. (e) Remanent magnetization at $t=20$ s as a function of temperature: gray solid line corresponds to the constant distance between the borders of magnetic units of 9 Å while the black one to the uniform border-border separation from the interval 8–13 Å. Both curves are for $K=50$ meV.

$\times10^4$ μm^{-2} and the total magnetic moment of an unit is $3000\mu_B$. Estimated value of the MAE, K is assumed to be about 50 meV (Ref. 45) but we also tested cases of $K=30$ (Ref. 7), 70, and 90 meV. Different randomly generated layouts of magnetic units were used in different Monte Carlo runs. The quasirandom distribution of magnetic units we deal with ($\simeq$20%—no neighbors, $\simeq$40%—one neighbor, and $\simeq$40%—two and more neighbors) reasonably fits the experimental one (see Sec. II D). An example of such a distribution is presented in Fig. 5(a). The exchange interaction J of the Hamiltonian (1) is set to 50 meV, according to the results of Sec. II C. We neglect the vanishing exchange interaction between non-neighbor units [Fig. 1(b)] because the separation between the borders of such magnetic units exceeds 1.5 nm.

Within our kMC simulations we are interested in two aspects of magnetic behavior of ensembles of magnetic units. We study (i) remanent magnetization of the ensemble, which has been initially magnetized along its easy axis and (ii) the magnetic behavior in the periodically oscillating external magnetic field. Figure 5(b) demonstrates the results of the kMC simulations of the relative remanent magnetization m_r/m_s of the dot ensemble as a function of the temperature. The starting magnetization m_s was achieved by preliminarily applied magnetic field, which then was switched off at $t=0$. The remanent magnetization m_r was measured at $t=20$ s.[46] Each data point of Fig. 5(b) was calculated by averaging over 500 of independent runs to reduce possible errors. For different kMC runs different quasirandom geometrical arrangements of clusters has been generated.

In the absence of the exchange interaction between nanodots ($J=0$) the ferromagnetic behavior is caused only by the MAE of individual particles. The corresponding remanent magnetization [plotted in Fig. 5(b) with dashed curves] vanishes to zero at $\simeq$15, 25, 35, and 45 K for $K=30$, 50, 70, and 90 meV, respectively. If the exchange interaction is "switched on," remanent magnetization preserves up to about 120, 130, 140, and 150 K for the same values of K. Thus the blocking temperature of this system enhanced by $\simeq$100 K is induced by the indirect exchange coupling between magnetic units.

The observed magnetism of the nanodot ensemble remains quite stable with time. Figure 5(c) demonstrates time-dependent remanent magnetization for the case $K=50$ meV at three different temperatures: 60, 80, and 100 K. One can see that first the magnetization falls rapidly. This happens due to the nanodots, which have no neighbors or small number of neighbors within the ensemble. After that the magnetization remains almost unchanged, due to the nanodots which have large number of neighboring magnetic units.[46] Hysteresis loops for the magnetic units ensemble for $K=50$ meV at different temperatures are demonstrated in Fig. 5(d).[47] At $T=60$ K the coercive field equals to 170 Oe. At $T=80$ K the coercive field is 50 Oe and at $T=100$ K it is 20 Oe. The hysteresis loops similar to the remanent magnetization curves at the corresponding value of K also indicate on a blocking temperature of $\simeq$130 K. We also plot in Fig. 5(d) the hysteresis loop calculated for $J=0$ meV. One can see the paramagnetic S-like curves already at $T=60$ K.

It is important to note that the remanent magnetization curve and the blocking temperature of an ensemble of magnetic units is quite sensitive to the dot-dot separation distribution and thus to the distribution of J within the ensemble. To illustrate this we consider the same quasirandom distribution as before, i.e., with $\simeq$20% of units without neighbors, $\simeq$40%—with one neighbor, and $\simeq$40%—with two and more neighbors. But now we assume that the separation between the dots borders is uniformly distributed in the interval 8–13 Å, which corresponds to the range of the most probable separations derived from the long-range interaction between two Fe nanoclusters (Fig. 4).[48] The remanent magnetization curve computed for such a unit-unit distribution for $K=50$ meV is shown in Fig. 5(e) with black curve. It is compared with the corresponding curve for the case of quasirandom distribution with the fixed border-border separation of 9 Å [the gray solid curve from Fig. 5(b)]. Due to the various separations between the dots borders, J is not a constant within an ensemble and the blocking temperature is $\simeq$90 K vs $\simeq$130 K for the constant border-border distance of 9 Å.

IV. CONCLUSIONS

In conclusion, we have theoretically investigated collective ferromagnetism in the ensembles of Fe nanoclusters. By the example of Fe nanoclusters (and nanodots) on Cu(111),

we have unambiguously demonstrated that the substrate-mediated interaction could be strong enough to induce the magnetic ordering only if several conditions are satisfied: (i) the nanoclusters should be partially embedded into the substrate to increase the density of confined conduction electrons; (ii) the distance between borders of neighboring nanoclusters should be chosen to produce a strong confinement of conduction electrons; (iii) the intrinsic structure of magnetic nanocluster should promote a good reflectivity of conduction electrons. The kMC simulations based on the Ising-type model for magnetization dynamics have shown that such conditions result in the enhanced blocking temperatures.

ACKNOWLEDGMENT

This work is supported by Deutsche Forschungsgemeinschaft (SPP1165 and SPP1153).

*stepanyu@mpi-halle.mpg.de

[1] J. V. Barth, G. Costantini, and K. Kern, Nature (London) **437**, 671 (2005).
[2] J. Shen, R. Skomski, M. Klaua, H. Jenniches, S. S. Manoharan, and J. Kirschner, Phys. Rev. B **56**, 2340 (1997).
[3] P. Gambardella, A. Dallmeyer, K. Maiti, M. C. Malagoli, W. Eberhardt, K. Kern, and C. Carbone, Nature (London) **416**, 301 (2002).
[4] J. Shen, J. P. Pierce, E. W. Plummer, and J. Kirschner, J. Phys.: Condens. Matter **15**, R1 (2003).
[5] F. Meier, L. Zhou, J. Wiebe, and R. Wiesendanger, Science **320**, 82 (2008).
[6] P. Gambardella, S. Rusponi, T. Cren, N. Weiss, and H. Brune, C. R. Phys. **6**, 75 (2005).
[7] S. Rohart, V. Repain, A. Tejeda, P. Ohresser, F. Scheurer, P. Bencok, J. Ferre, and S. Rousset, Phys. Rev. B **73**, 165412 (2006).
[8] G. Ballentine, M. Heßler, M. Kinza, and K. Fauth, Eur. Phys. J. D **45**, 535 (2007).
[9] M. Hillenkamp, G. Di Domenicantonio, and C. Félix, Phys. Rev. B **77**, 014422 (2008).
[10] M. R. Scheinfein, K. E. Schmidt, K. R. Heim, and G. G. Hembree, Phys. Rev. Lett. **76**, 1541 (1996).
[11] A. Sugawara and M. R. Scheinfein, Phys. Rev. B **56**, R8499 (1997).
[12] S. Bedanta, T. Eimüller, W. Kleemann, J. Rhensius, F. Stromberg, E. Amaladass, S. Cardoso, and P. P. Freitas, Phys. Rev. Lett. **98**, 176601 (2007).
[13] P. Poulopoulos, P. J. Jensen, A. Ney, J. Lindner, and K. Baberschke, Phys. Rev. B **65**, 064431 (2002).
[14] J. P. Pierce, M. A. Torija, Z. Gai, J. Shi, T. C. Schulthess, G. A. Farnan, J. F. Wendelken, E. W. Plummer, and J. Shen, Phys. Rev. Lett. **92**, 237201 (2004).
[15] M. A. Torija, A. P. Li, X. C. Guan, E. W. Plummer, and J. Shen, Phys. Rev. Lett. **95**, 257203 (2005).
[16] D. Altbir, J. d'Albuquerque e Castro, and P. Vargas, Phys. Rev. B **54**, R6823 (1996).
[17] R. Skomski, Europhys. Lett. **48**, 455 (1999).
[18] R. Skomski, J. Zhang, V. Sessi, J. Honolka, A. Enders, and K. Kern, J. Appl. Phys. **103**, 07D519 (2008).
[19] V. N. Kondratyev and H. O. Lutz, Phys. Rev. Lett. **81**, 4508 (1998).
[20] A. F. Bakuzis, A. R. Pereira, J. G. Santos, and P. C. Morais, J. Appl. Phys. **99**, 08C301 (2006).
[21] W. C. Lin, Z. Gai, L. Gao, J. Shen, P. J. Hsu, H. Y. Yen, and M. T. Lin, Phys. Rev. B **80**, 024407 (2009).
[22] R. Zeller, P. H. Dederichs, B. Újfalussy, L. Szunyogh, and P. Weinberger, Phys. Rev. B **52**, 8807 (1995).
[23] K. Wildberger, V. S. Stepanyuk, P. Lang, R. Zeller, and P. H. Dederichs, Phys. Rev. Lett. **75**, 509 (1995).
[24] V. S. Stepanyuk, W. Hergert, K. Wildberger, R. Zeller, and P. H. Dederichs, Phys. Rev. B **53**, 2121 (1996).
[25] N. Papanikolaou, R. Zeller, and P. H. Dederichs, J. Phys.: Condens. Matter **14**, 2799 (2002).
[26] V. S. Stepanyuk, A. N. Baranov, D. V. Tsivlin, W. Hergert, P. Bruno, N. Knorr, M. A. Schneider, and K. Kern, Phys. Rev. B **68**, 205410 (2003).
[27] J. Zabloudil, R. Hammerling, L. Szunyogh, and P. Weinberger, *Electron Scattering in Solid Matter*, Springer Series in Solid-State Sciences Vol. 147 (Springer-Verlag, Berlin, 2005).
[28] P. Lang, L. Nordström, K. Wildberger, R. Zeller, P. H. Dederichs, and T. Hoshino, Phys. Rev. B **53**, 9092 (1996).
[29] V. S. Stepanyuk, L. Niebergall, W. Hergert, and P. Bruno, Phys. Rev. Lett. **94**, 187201 (2005).
[30] O. O. Brovko, P. A. Ignatiev, V. S. Stepanyuk, and P. Bruno, Phys. Rev. Lett. **101**, 036809 (2008).
[31] A. Hernando, F. Briones, A. Cebollada, and P. Crespo, Physica B **322**, 318 (2002).
[32] M. Jamet, W. Wernsdorfer, C. Thirion, V. Dupuis, P. Mélinon, A. Pérez, and D. Mailly, Phys. Rev. B **69**, 024401 (2004).
[33] J. Bansmann, M. Getzlaff, A. Kleibert, F. Bulut, R. K. Gebhardt, and K. H. Meiwes-Broer, Appl. Phys. A: Mater. Sci. Process. **82**, 73 (2006).
[34] M. Klaua, H. Höche, H. Jenniches, J. Barthel, and J. Kirschner, Surf. Sci. **381**, 106 (1997).
[35] R. C. Longo, V. S. Stepanyuk, W. Hergert, A. Vega, L. J. Gallego, and J. Kirschner, Phys. Rev. B **69**, 073406 (2004).
[36] J. Repp, F. Moresco, G. Meyer, K.-H. Rieder, P. Hyldgaard, and M. Persson, Phys. Rev. Lett. **85**, 2981 (2000).
[37] N. Knorr, H. Brune, M. Epple, A. Hirstein, M. A. Schneider, and K. Kern, Phys. Rev. B **65**, 115420 (2002).
[38] S. U. Nanayakkara, E. C. H. Sykes, L. C. Fernández-Torres, M. M. Blake, and P. S. Weiss, Phys. Rev. Lett. **98**, 206108 (2007).
[39] G. Manai, K. Radican, F. Delogu, and I. V. Shvets, Phys. Rev. Lett. **101**, 165701 (2008).
[40] M. Gabl, M. Bachmann, N. Memmel, and E. Bertel, Phys. Rev. B **79**, 153409 (2009).
[41] Y. Li and B.-G. Liu, Phys. Rev. B **73**, 174418 (2006).
[42] R. J. Glauber, J. Math. Phys. **4**, 294 (1963).
[43] N. Metropolis, A. W. Rosenbluth, M. N. Rosenbluth, A. H. Teller, and E. Teller, J. Chem. Phys. **21**, 1087 (1953).
[44] K. A. Fichthorn and W. H. Weinberg, J. Chem. Phys. **95**, 1090

(1991).

[45] This is a reasonable value since the typical value of a MAE of a surface Fe atom in an Fe-bulk particle is 0.4 meV (Ref. 32) and the number of surface Fe atoms in a particle having hemisphere shape and containing 800 atoms (Ref. 15) is about 120.

[46] We have chosen time interval of $t=20$ s since it is realistic time known from the experiments [see Fig. 1(c) in Ref. 14]. Our calculations demonstrate that the remanent magnetization is almost unchanged on the time scale of 10–100 s. In principle, the magnitude of the remanent magnetization depends on the moment of time t, when it is measured. With increasing t at a given T the value of remanent magnetization decreases and in the limit of infinite t it drops to zero at any T (i.e., there is no convergence of remanent magnetization).

[47] In our simulations we have considered that the sweeping rate of external magnetic field is 0.01 T/sec, i.e., close to the experimental setup (Ref. 2).

[48] If the separation between the borders of magnetic units is 9 Å, then J is considered to be 50 meV. Otherwise it is rescaled according to the data shown in Fig. 1(b).